Journal of the Geological Society, London, Vol. **160**, 2003, pp. 71–82. Printed in Great Britain.

Fractionation of carbon and oxygen isotopes in ^{13}C-rich Palaeoproterozoic dolostones in the transition from medium-grade to high-grade greenschist facies: a case study from the Kola Superdeep Drillhole

VICTOR A. MELEZHIK[1], ANTHONY E. FALLICK[2], YURY P. SMIRNOV[3] & YURY N. YAKOVLEV[3]

[1]*Geological Survey of Norway, Leiv Eirikssons vei 39, N-7491 Trondheim, Norway (e-mail: victor.melezhik@ngu.no)*

[2]*Scottish Universities Environmental Research Centre, East Kilbride, Glasgow G75 0QF, UK*

[3]*Scientific Industrial Centre 'Kola Superdeep', 184415 Zapolyarny, Russia*

Abstract: Samples from the Kola Superdeep Drillhole (12 262 m), a deep drillhole (1060 m), and from the surface, seaprated by only around 10 km, provided a unique opportunity for direct tracing of δ^{13}C and δ^{18}O changes through a low- to high-grade greenschist-facies transition within impure, ^{13}C-rich Palaeoproterozoic dolostones. The least-altered dolostones have δ^{13}C of +9‰ and δ^{18}O of 22‰. The metamorphic transition is expressed by dolomite + calcite$_1$ + quartz ± K-feldspar → tremolite + calcite$_2$ ± dolomite ± calcite$_1$ and defined by ^{13}C depletion of calcite$_2$ (*c*. 3.0‰), calcite$_1$ (1.0–2.0‰) and dolomite (<1‰) which is associated with a Rayleigh distillation process. δ^{18}O shows a considerable resetting in all carbonate components by around 6‰ caused by a Rayleigh distillation process coupled with isotopic exchange between the carbonates and fluids with an external source of oxygen. The retrograde alteration is expressed by the formation of quartz–chlorite veinlets within tectonically bound zones of brecciated and sheared dolostones. The maximum ^{18}O depletion in dolomite (9‰) and calcite$_1$ (*c*. 4‰) were probably controlled by infiltration into permeable zones of external fluids associated with retrograde alteration; δ^{13}C remains largely unaffected.

Keywords: Kola Superdeep Drillhole, Palaeoproterozoic, dolomite, calcite, stable isotopes.

Screening of carbon and oxygen isotope values of carbonates for diagenetic and metamorphic alterations is an obligatory procedure when investigating stratigraphic variations in δ^{13}C and δ^{18}O. The variables that control the isotopic composition of metamorphic carbonates include the composition of the original sediment and fluid, fluid/rock ratio, porosity, fractionation factors, distribution coefficients and open-system v. closed-system behaviour (Banner & Hanson 1990). Theoretical considerations of the trace element geochemistry that may predict post-depositional resetting of δ^{13}C and δ^{18}O in sedimentary carbonates have been considered and systematized byVeizer (1983a, 1983b, and later revisions). This trace element approach has been successfully used in numerous isotopic studies of Precambrian carbonates (Veizer *et al*. 1990, 1992a, 1992b).

In the absence of aluminous silicates, even high-grade marbles may retain essentially depositional δ^{13}C values (Taylor & O'Neil 1977; Valley & O'Neil 1984; Ghent & O'Neil 1985; Baker & Fallick 1989a, 1989b; Wickham & Peters 1993; Melezhik *et al*. 2001). Zheng (1997) reported a case where marbles subducted to mantle depth may have retained their syndepositional δ^{13}C values. In the presence of quartz and/or feldspar, the C- and O-isotopic composition of carbonate minerals is commonly altered by re-equilibration with metamorphic fluids or by metamorphic decarbonation reactions (e.g. Shieh & Taylor 1969; Valley 1986). Partial resetting of the oxygen isotopic system would result in an O/C trend paralleling the oxygen axis. Complete δ^{13}C and δ^{18}O equilibration with fluids during metamorphism commonly results in a non-linear δ^{13}C/δ^{18}O alteration trend (Nabelek 1991). Large ^{13}C and ^{18}O depletions have been reported from greenschist-facies carbonate rocks affected by strong deformation (Guerrera *et al*. 1997).

In recent years stable isotope systematics have been relatively well understood and quantified from contact metamorphism, whereas theoretical consideration of the carbon and oxygen isotope re-equilibration related to regional metamorphism presents a more difficult problem (Valley 1986; Baumgartner & Valley 2001). In most cases, the degree of metamorphic resetting of C and O isotopes associated with regional metamorphic transformations cannot be quantitatively measured, because of the great difficulties in precise stratigraphic correlation between low- and high-grade rocks in regionally metamorphosed and deformed terranes.

The Kola Superdeep Drillhole in NW Russia (Fig. 1), the deepest by far in the world (12 262 m), offers a unique opportunity for making a comparative study of Palaeoproterozoic carbonate rocks that underwent progressive regional metamorphism. In this case, the assessment of isotopic resetting can be made within the same formation based on comparison between the biotite-actinolite-facies dolostones exposed on the surface and the epidote-amphibolite-facies dolostones intersected by the Superdeep Drillhole (Figs 2 and 3). Access to extensive stratigraphic sections of the same formation in a nearby 1060 m deep drillhole (drillhole X) is an additional asset. The transition within a limited *PT* range, from low- to high-grade greenschist conditions, is expected to be a key thermodynamic regime where most decarbonation reactions start (e.g. Winkler 1979). The metamorphic transition occurs over a rather limited distance of around 10 km (Fig. 2) within the same depositional basin and within the same carbonate lithology (Fig. 4). This is, therefore, one of those rare cases when the interference of differences in depositional settings and mineralogical precursors of the rocks involved in the comparison can be radically minimized. Additionally, the Palaeoproterozoic formation chosen for this investigation represents one of the key localities in the study of ^{13}C-rich dolostones occurring world-wide and representing one of the greatest positive isotopic shifts of $\delta^{13}C_{carb}$ and a series of associated first-

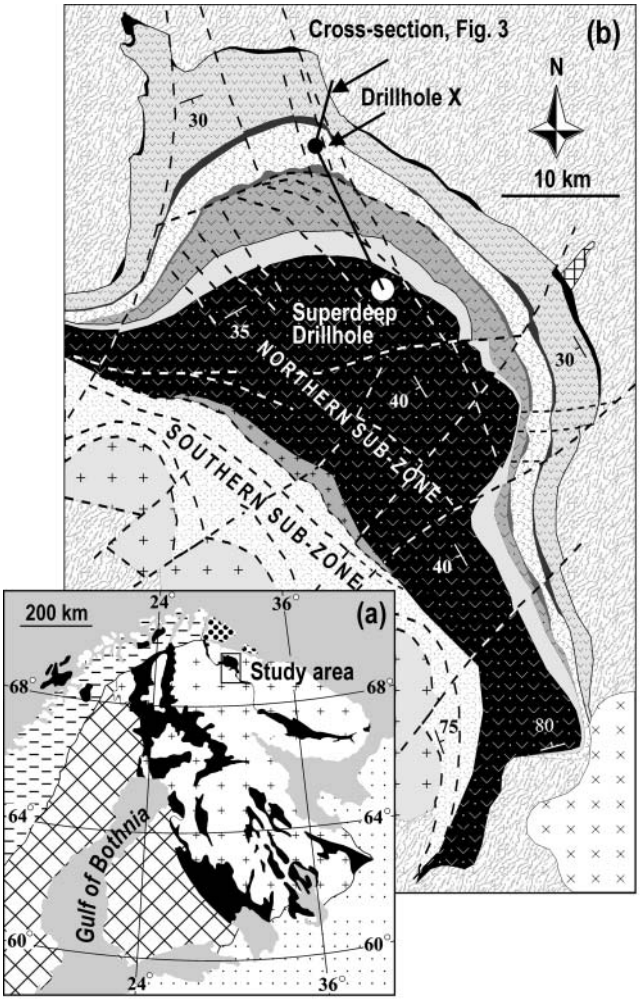

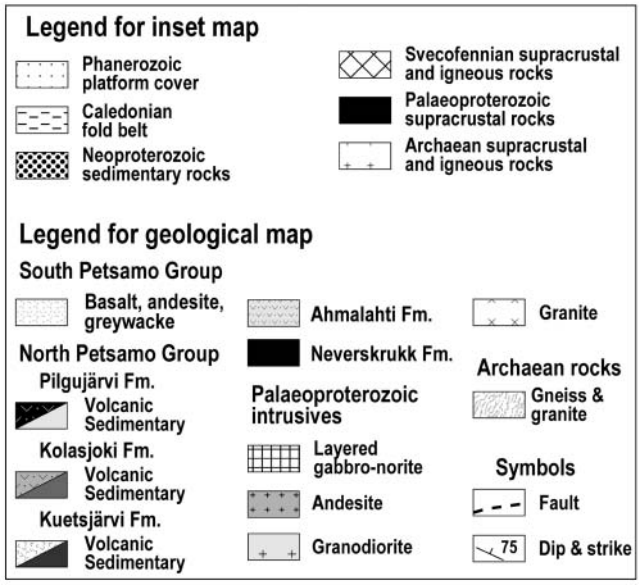

Fig. 1. (**a**) Geographical and geological location of the study area (inset map); (**b**) simplified geological map of the Pechenga Greenstone Belt. Geological map is from Zagorodny *et al*. (1964) modified by Melezhik *et al*. (1995).

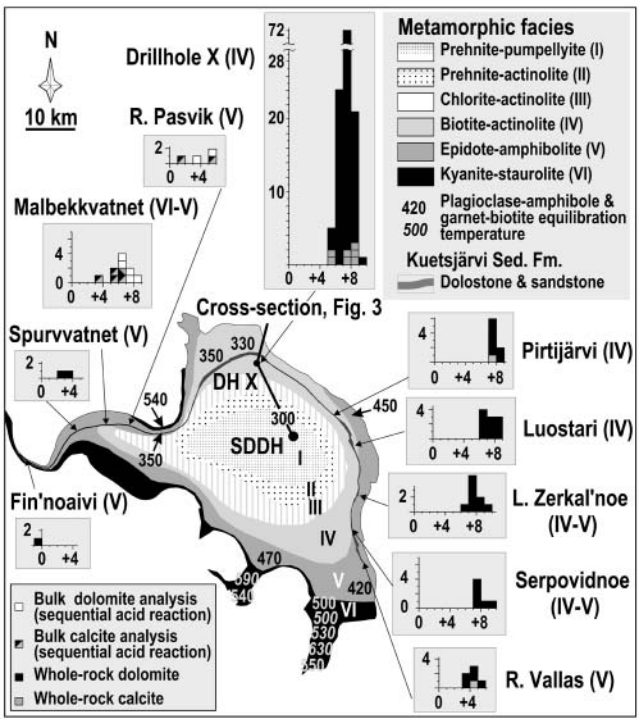

Fig. 2. Metamorphic zoning of the Pasvik–Pechenga Greenstone Belt (modified from Petrov & Voloshina 1995); location of sampling sites; and histograms of $\delta^{13}C_{carb}$ values obtained from the Kuetsjärvi carbonates by previous studies (Melezhik & Fallick 1996). SDDH, Superdeep Drillhole; DH X, Drillhole X.

order palaeoenvironmental transformations in the Earth's history (e.g. Melezhik *et al*. 1999).

Thus, this paper will address two problems of fundamental importance, namely, the scale of carbon and oxygen isotope fractionation in regionally metamorphosed dolostones; and metamorphic impact on carbon and oxygen isotope values in the dolostones representing the greatest global episode of perturbation of the terrestrial carbon cycle. Both problems are current challenges.

The main objectives of this research are (1) to define the magnitude of carbon and oxygen isotope fractionation in the transition from low-grade to high-grade greenschist facies within a limited *PT* range; (2) to obtain a better insight into the degree of carbon and oxygen isotope resetting in greenschist-facies ^{13}C-rich dolostones; (3) to discriminate between regional (metamorphism) and local (post-peak-metamorphic shearing) factors causing $\delta^{13}C$ and $\delta^{18}O$ variations.

Geological background

The dolostone unit chosen for the isotopic study is a part of the Kuetsjärvi Sedimentary Formation (Zagorodny *et al*. 1964), which belongs to the Palaeoproterozoic Pechenga–Pasvik Greenstone Belt, Kola Peninsula, NW Russia (Fig. 1a). Structurally the Pechenga–Pasvik Belt is composed of two sub-zones (Fig. 1b). The Northern Sub-Zone is a simple half-graben filled with predominantly volcanic rocks gently dipping 10–40° southwards, whereas the Southern Sub-Zone is tectonically imbricated nappes overthrust by Archaean rocks (Fig. 1b).

The rocks of the Pechenga–Pasvik Belt comprise the Petsamo

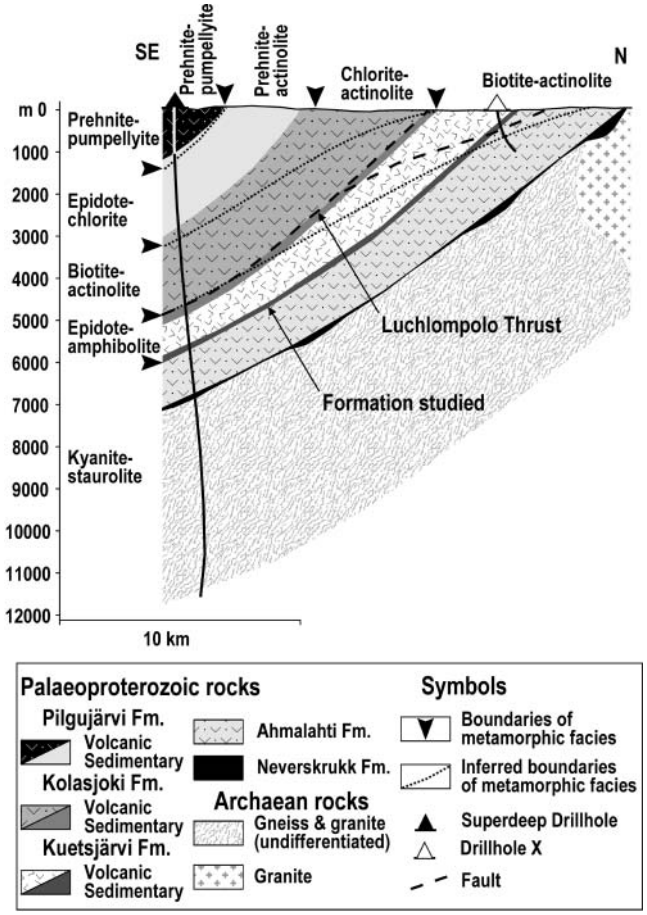

Fig. 3. Lithostratigraphic section through the Kola Superdeep Drillhole (modified from Lanev *et al*. 1987). Boundaries of the metamorphic facies between the Superdeep Drillhole (Glagolev *et al*. 1987) and the surface (modified from Petrov & Voloshina 1995) are inferred.

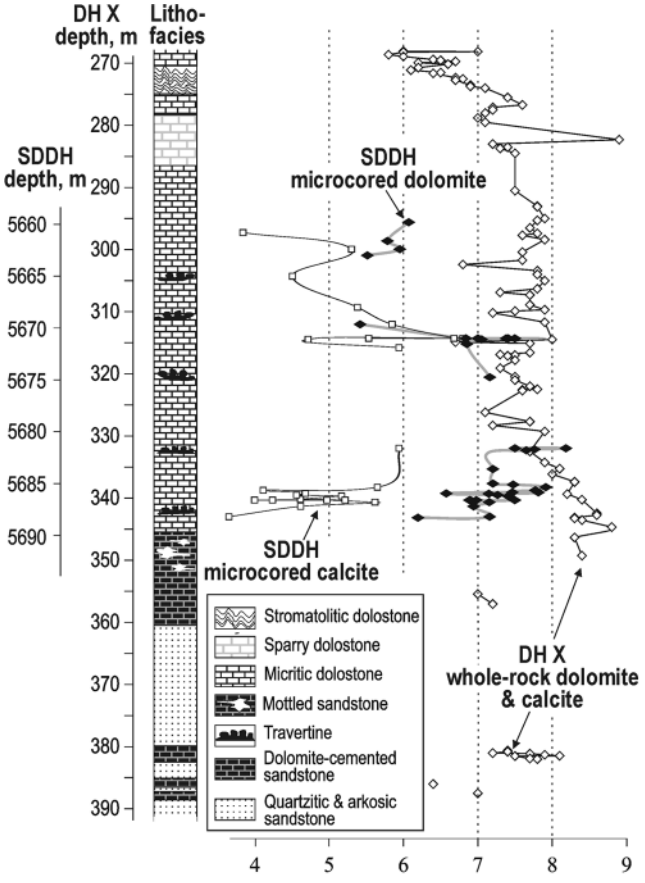

Fig. 4. $\delta^{13}C_{carb}$ v. stratigraphy. It should be noted that dolomite and calcite from the Superdeep Drillhole (epidote-amphibolite metamorphic facies) are considerably depleted in ^{13}C compared with those from drillhole X (biotite-actinolite metamorphic facies). Data from drillhole X are from Melezhik & Fallick (1996).

Supergroup, which is subdivided into the North Petsamo Group and South Petsamo Group. The 120 m thick Kuetsjärvi Sedimentary Formation is one of the stratigraphic units comprising the North Petsamo Group. The cumulative stratigraphic thicknesses of the sedimentary and volcanic rocks of the group are 1600 m and 12 000 m, respectively.

From a palaeotectonic point of view the Pechenga–Pasvik Greenstone Belt is a long-lived (from 2.5 to 1.8 Ga) intracontinental rift, which developed into an intercontinental rift with a subsequent aborted oceanic phase (e.g. Marker 1985; Mintz 1993; Melezhik & Sturt 1994; Sharkov & Smolkin 1997). The lower age limit of the North Pechenga Group is constrained by inclusions in the basal conglomerates of gabbro–norite pebbles (Bakushkin & Akhmedov 1975), which are derived from the layered intrusion dated to 2505 ± 1.6 Ma (U–Pb zircon, Amelin *et al*. 1995). The upper age limit of the group is younger than 1970 ± 5 Ma (U–Pb zircon, Hanski *et al*. 1990) obtained from rhyolitic tuffs of the Pilgujärvi Volcanic Formation (Fig. 1b). The age of the Kuetsjärvi Sedimentary Formation is bracketed between 2324 ± 28 and 2214 ± 54 Ma by the Rb–Sr whole-rock analyses on volcanites (Balashov 1996).

Regional metamorphism and deformation

All geological formations in the Pechenga–Pasvik Belt have been affected by the Svecofennian polyphase orogenic deformation (Duk 1977). The rocks underwent zoned, regional metamorphism grading from prehnite–pumpellyite facies in the central part of the Pechenga Belt to amphibolite facies towards the peripheral zones (Petrov & Voloshina 1995). Six metamorphic zones have been recognized based on metamorphic mineral parageneses (Fig. 2). In general, prograde regional metamorphism characterized the first two deformational phases (D_1 and D_2), with the peak staurolite-grade event attained during the second main deformation (D_2). Based on previous studies from eastern part of the Pechenga–Pasvik Belt (e.g. Petrov & Voloshina 1995), peak temperatures were 500–650 °C and pressure was around 520–900 MPa. The age of this peak metamorphism has been poorly constrained at *c*. 1850 Ma (e.g. Balashov 1996). The cooling history of the Pechenga–Pasvik Belt rocks has not been constrained.

In the northern part of the Pechenga zone, in the vicinity of drillhole X (Fig. 1), megascopic signs of the early deformation (D_1) are absent in the Kuetsjärvi Sedimentary Formation, and the oldest tectonic fabric belongs to the ESE system of folds (D_2). This is a relatively weak deformation with only limited and sporadic development of cleavage and folding and a gentle southwards tilting. The sporadic D_2 cleavage is a rough-spaced cleavage, developed in bands of siltstones. In the Superdeep Drillhole rocks D_1 is clearly expressed as schistosity (S_1) developed subparallel to primary bedding (S_0). The tectonic fabric belonging to D_2 is a pervasive, oblique cleavage defined by

dimensional orientation of clasts and emphasized by the effects of pressure solution or seams of insoluble residue. D_1 was associated with burial metamorphism whereas D_2 marked a peak-metamorphic event and a NNE-directed major overthrusting by a southern Archaean terrane (Melezhik & Sturt 1995).

A later extensional event (D_3) caused a retrograde, post-peak-metamorphic, syntectonic fabric. This is expressed by brecciation, recrystallization and formation of low-temperature quartz–chlorite veinlets. The retrograde metamorphism and associated fabric and alteration are bound to major thrust zones (e.g. the Luchlompolo Thrust, Fig. 3) and affected rocks within several fault-bound transversal blocks.

On the present-day erosional surface, boundaries of the six metamorphic zones are sub-concordant with the formational boundaries in the central Northern Sub-Zone whereas they have a clear cross-cutting relationship in the NW and SE flanks of the belt, thus showing concentric development (Fig. 2). Similar metamorphic zones, as well as a vertical metamorphic zoning, have been documented in the Superdeep Drillhole, which intersected the entire North Petsamo Group sequence (Fig. 3) starting from the lower part of the Pilgujärvi Volcanic Formation (Fig. 1b). The prehnite–pumpellyite facies extends from the surface to a depth of 1400 m. The boundary between the biotite-actinolite and epidote-amphibolite facies has been recognized at a depth of 4900 m, whereas the amphibolite facies begins at about 6000 m and extends to 12 262 m (Glagolev *et al*. 1987). In the central Northern Sub-Zone, all metamorphic zones dip gently southwards and cross-cut, at an oblique angle, steeper stratigraphic boundaries (Fig. 3).

Sampling sites with respect to metamorphic zoning

In the central Northern Sub-Zone, on the present-day erosional surface, the Kuetsjärvi Sedimentary Formation is developed in the biotite-actinolite metamorphic facies, and it gradually passes into the epidote-amphibolite facies in the western and eastern flanks of the zone (Fig. 2). Two sampling sites (Pirtjärvi and Luostary) are located in the biotite-actinolite metamorphic facies, three others (Malbekkvatnet, Zerkal'noe and Serpovidnoe) are in the transition to the epidote-amphibolite facies, and four (Fin'-noaivi, Spurvvatnet, Pasvik and Vallas) are in the epidote-amphibolite facies (Fig. 2). All these sampling sites are natural outcrops and man-made quarries, and thus do not represent the entire formational thickness of the stratigraphic unit.

Another sampling site from the biotite-actinolite metamorphic facies is represented by the 1060 m deep drillhole X in the central Northern Sub-Zone (Figs 1b, 2, 3 and 4). Samples have been collected from the depth interval 267–395 m. Good drillcore recovery allowed high-density sampling through the entire formational thickness (Melezhik & Fallick 1996). Although all drillcore material is from the biotite-actinolite facies (Fig. 3), the geological environment of drillhole X differs from that of other sampling sites of similar metamorphic grade: drillhole X intersected partially sheared and brecciated rocks within a narrow NW–SE-trending block bounded by faults (Fig. 1b). These faults are connected to one of the major fault zones (the Luchlompolo Thrust, Fig. 3) and thus define a relatively permeable zone. The D_3 shearing and brecciation is accompanied by sporadic development of low-temperature chlotite and quartz–chlorite veinlets that post-date the peak metamorphism.

Samples of carbonate rocks representing a higher, epidote-amphibolite grade have been obtained from Superdeep Drillhole. Samples have been collected from the depth interval 5647–5708 m (Figs 3 and 4). As a result of low core recovery, the sampling was rather biased. Dense sampling has been possible from only two depth intervals, namely 5668–5672 and 5681–5688 m.

Analytical techiques

Submilligram microsamples for oxygen and carbon isotope analyses were obtained using a Ulrike Medenbach microcorer. The microsamples were cored from 150 mm thick polished sections stained with alizarin-red. The major and trace elements were analysed by XRF at the Geological Survey of Norway using a Philips PW 1480 X-ray spectrometer. The accuracy (1σ) is typically better than 2% of the oxide present (SiO_2, Al_2O_3, MgO, CaO), even at the level of 0.05 wt%, and the precision is almost invariably higher than the accuracy. The analytical uncertainties (1σ) for Sr, MnO and Fe_2O_3 are better than ± 5.5 ppm, $\pm 0.003\%$ and $\pm 0.01\%$, respectively.

Oxygen and carbon isotope analyses of microcores were carried out at Scottish Universities Environmental Research Centre using the phosphoric acid method of McCrea (1950) modified for operation at 90 °C with a VG PRISM + ISOCARB mass spectrometer. Oxygen isotope data were corrected using a calcite-CO_2 fractionation factor of 1.00793. For dolomite-CO_2 we interpolated data given by Rosenbaum & Sheppard (1986) to obtain 1.00932. The $\delta^{13}C$ data are reported in per mil (‰) relative to V-PDB and the $\delta^{18}O$ data in per mil relative to V-SMOW. Precision and accuracy for isotopically homogeneous material are better than ± 0.1‰ (1σ)

Chemical composition and mineral parageneses of carbonate rocks

The Kuetsjärvi Sedimentary Formation carbonate rocks are mainly sandy dolostone with very few thin beds of limestone. Both the dolostones and the limestones are enriched in SiO_2. Concentration of Al_2O_3 (1.5–7.5%) and K_2O (2–4%) can be significant in those samples containing sericite and clastic muscovite (Table 1). The carbonate rocks from the surface and drillhole X are geochemically indistinguishable. There is, however, a major difference in chemical composition of the carbonate rocks collected from the Superdeep Drillhole sections: many of them are significantly depleted in CO_2 and alkalis (Table 1). All rocks are devoid of organic matter.

Primary mineral parageneses of dolostones are represented by dolomite + quartz + sericite ± K-feldspar ± $calcite_1$. The metamorphic parageneses in the biotite-actinolite facies are theoretically defined by the reaction: 3 dolomite + 4 quartz + 1 $H_2O \rightarrow$ 1 talc + 3 $calcite_2$ + 3 CO_2 (e.g. Winkler 1979). Talc has been observed in the biotite-actinolite-facies dolostones of the Kuetsjärvi Sedimentary Formation; however, it is not common.

The metamorphic paragenesis observed in the epidote-ampibolite-facies dolostones is defined by tremolite + $calcite_2$. The formation of tremolite was due to a well-known reaction: 5 dolomite + 8 quartz + 1 $H_2O \rightarrow$ 1 tremolite + 3 $calcite_2$ + 7 CO_2 (e.g. Winkler 1979). However, quartz deficiency with respect to dolomite for the production of tremolite commonly resulted in the formation of the tremolite + $calcite_2$ + dolomite paragenesis. Therefore three main mineral parageneses are present in the epidote-ampibolite facies: (1) dolomite + $calcite_1$ (Fig. 5a); (2) tremolite + $calcite_2$ + dolomite (Fig. 5b); (3) tremolite + $calcite_2$ (Fig. 5c). Thus the dolostones from the epidote-ampibolite facies may contain two generations of calcite, namely pre-metamorphic calcite ($calcite_1$) and metamorphic calcite ($calcite_2$). These two generations of calcite have been distinguished by mineralogical criteria. $Calcite_1$ occurs in the form of isomorphic crystals which make up 0.2–1.5 cm thick

Table 1. *Chemical composition of the Kuetsjärvi carbonate rocks (oxides in %)*

Sample number	Mineralogical composition	Depth (m)	SiO_2	Al_2O_3	Fe_2O_3	MnO	MgO	CaO	Na_2O	K_2O	P_2O_5	CO_2	CO_2 lost
Surface (biotite-actinolite facies)													
188	Sandy dolostone		13.7	0.90	0.73	0.04	14.0	30.7	0.10	0.81	n.d	38.9	1.2
350	Sandy dolostone		25.0	5.3	2.9	0.14	10.1	22.7	0.19	3.2	0.06	30.4	8.3
400	Dolomite-cemented quartz sandstone		50.8	0.60	0.85	0.03	10.4	15.4	0.35	0.07	n.d	21.5	8.3
504	Sandy dolostone		42.8	0.24	1.36	0.04	11.9	18.0	0.04	0.24	n.d	25.4	6.3
505	Sandy dolostone		16.0	1.79	0.95	0.04	17.5	25.5	0.05	0.60	0.07	37.6	4.0
506	Sandy dolostone		15.6	0.13	0.06	–	18.9	26.9	0.02	0.18	n.d	38.2	8.4
Drillhole X (biotite-actinolite facies)													
268.6	Sandy limestone with minor talc	268.6	31.7	1.52	0.46	0.11	3.2	34.8	0.01	0.05	0.03	28.0	9.0
295.3	Sandy dolostone with apatite and minor talc	295.3	31.0	1.20	0.78	0.05	14.8	21.2	0.02	0.52	0.34	30.1	8.1
310.2	Sandy dolostone	310.2	14.9	0.27	0.32	0.02	18.0	26.6	0.02	0.05	0.03	39.8	1.7
336.2	Sandy dolostone with minor talc	336.2	31.0	0.66	0.30	0.01	14.8	21.1	0.02	0.33	0.02	31.9	2.6
337.4	Sandy dolostone	337.4	19.7	0.64	0.32	0.03	15.2	27.4	–	0.36	0.04	36.2	4.9
381.2	Sandy dolostone with muscovite	381.2	42.5	3.50	0.85	0.02	12.3	16.9	0.05	1.95	0.03	21.8	18.2
Superdeep Drillhole (epidote-amphibolite facies)													
5647	Tremolite–calcite–dolomite rock	5647	23.0	1.22	0.60	0.13	17.5	28.9	–	–	0.02	28.7	31.3
5659	Tremolite–calcite–dolomite rock	5659	12.3	1.04	0.32	0.04	20.2	28.3	–	0.02	–	38.0	14.1
5662.7	Tremolite–calcite–dolomite rock	5662.7	17.6	1.06	0.34	0.03	19.7	26.9	–	0.02	0.03	34.6	18.8
5668	Tremolite–calcite–dolostone rock with talc and phlogopite	5668	34.8	1.15	0.46	0.04	20.1	24.8	–		–	18.9	54.3
5671.55	Dolostone	5671.55	5.5	0.41	0.33	0.04	22.5	28.9	–	–	–	42.4	10.2
5671.7	Tremolite–calcite–dolomite rock	5671.7	48.8	1.15	1.29	0.04	22.5	19.0	–	0.03	–	7.4	81.3
5687	Tremolite–calcite–dolomite rock with phlogopite	5687	41.8	2.36	0.59	0.02	21.2	20.9	–	0.27	–	13.0	67.1

CO_2 lost is shown in percent. It is calculated based on deficiency of CO_2 necessary to balance MgO and CaO. Sample numbers for drillhole X and Superdeep Drillhole refer to the depth from which the samples were collected.–, below detection limit, 0.02 wt%.

lenses and layers interbedded with thicker layers of dolomite (Fig. 5a). $Calcite_2$ is scattered within tremolite mass (Fig. 5b), where it commonly appears in the form of columnar crystals following the crystal morphology of the tremolite (Fig. 5c). In further discussion $calcite_1$ is referred to as 'primary' calcite, whereas $calcite_2$ is termed metamorphic calcite. However, both $calcite_1$ and dolomite, like $calcite_2$, have been recrystallized during metamorphic events. In several cases a third generation of calcite has been observed. This fills thin, open joints and is apparently associated with the latest (retrograde) event of the tectonometamorphic history. This calcite is designated as $calcite_3$.

Carbon and oxygen isotopes

Carbon and oxygen isotopes have been measured from bulk carbonate constituents in whole-rock samples (Table 2, 15 analyses) and from separate dolomite and calcite phases extracted by microcoring (Tables 3 and 4, 68 analyses). Additionally, 69 analyses from surface outcrops and 120 analyses from drillhole X have been incorporated from previous studies (Melezhik & Fallick 1996). Overall the $\delta^{13}C$ values range from -2.4 to $+8.9$‰, whereas $\delta^{18}O$ values span 7.3–20.4‰.

Within the biotite-actinolite facies the whole-rock dolomite samples from the surface and those sampled from the drillhole X section show similar $\delta^{13}C$ values, $+7.6 \pm 0.7$‰ (Fig. 6a) and $+7.4 \pm 0.6$‰ (Fig. 6b), respectively. Microcored dolomite samples within the epidote-amphibolite facies in Superdeep Drillhole give $+7.1 \pm 0.6$‰ (Fig. 6d). $\delta^{18}O$ values, however, differ in that the dolomite from the drillhole X section is depleted in ^{18}O (16.2 ± 2.7‰, Fig. 7b) relative to those sampled from outcrops (20.0 ± 0.8‰, see Fig. 7a) that are located outside the drilling site (Fig. 2). Although a $\delta^{18}O$ histogram shows a multimodal distribution of isotopic data, even the isotopically heaviest mode of the drillhole X samples (Fig. 7b) still shows a significant depletion in ^{18}O compared with the dolostones from the surface outcrops (Fig. 7a). A plot of $\delta^{18}O$ vs stratigraphy shows that in drillhole X the lowest values are associated with quartzite-hosted dolostone lenses (13.2–15.5‰, Fig. 8a), and particularly with those that are close to the contact with underlying basalts (11–11.5‰). There is a gradual $\delta^{18}O$ decrease from 18.2 to 13‰ over a distance of 6 m towards the contact with overlying basalts (Fig. 8a). A dolostone from the intensively brecciated zone has $\delta^{18}O$ of 13‰. The main dolostone body shows a symmetrical, gradual $\delta^{18}O$ decrease from the centre (19.5‰) towards the brecciated (17.5‰) and sheared zone with chlorite veinlets (17.0‰, Fig. 8a). Samples with $\delta^{18}O > 16.0$‰ are characterized by a significant, positive correlation between $\delta^{18}O$ and carbonate content ($r = 0.40$, $n = 67$). Samples with $\delta^{18}O$ O < 16.0‰, all from the contact zones, brecciated and sheared zones, and from the thin dolostone lenses hosted by quartzite, are marked by a different, less significant correlation ($r = 0.63$, $n = 12$, Fig. 8b).

$\delta^{18}O$ values obtained from the Superdeep Drillhole microcored dolomite show a significant depletion in ^{18}O (Fig. 7d); 2.7‰ on average with respect to the dolomite measured from the drillhole X section, and 6.5‰ compared with the dolomite obtained from the surface.

Similar ^{13}C depletion is recorded in calcite from the limestone sampled from an outcrop (+7.2‰, Fig. 6a), those collected from the drillhole X section ($+7.4 \pm 1.1$‰, $n = 7$, Fig. 6b), and the microcored Superdeep Drillhole $calcite_1$ ($+6.5 \pm 0.5$‰, $n = 6$, Fig. 6e). However, $\delta^{13}C$ measured from the microcored $calcite_2$ in the Superdeep Drillhole section is lower ($+4.8 \pm 0.7$‰, $n = 22$, Fig. 6e) and that of the vein-$calcite_3$ (-1.0‰) is the lowest of all (Fig. 6e). $\delta^{18}O$ values obtained from different calcites show two distinctive features. First, both $calcite_1$ (13.4 ± 0.5‰) and $calcite_2$ (14.0 ± 1.2‰) are similar. Second, excluding one sample, whole-rock calcite data from the biotite-actinolite facies in the drillhole X section plots on the histogram (Fig. 7) within a middle mode (14.4 ± 0.7‰, $n = 6$), and thus they are isotopically rather similar to the epidote-amphibolite-facies calcite in the Superdeep Drillhole section.

Carbon and oxygen isotope ratios measured from whole-rock samples in the epidote-amphibolite facies from the Superdeep Drillhole section show salient spread accompanied by a significant depletion in heavy isotopes (Table 2, Figs 6c and 7c). A few samples containing abundant vein-$calcite_3$ show $\delta^{13}C$ and $\delta^{18}O$ values below those of any their other carbonate components, i.e. dolomite, $calcite_1$ and $calcite_2$.

Discussion

The *c.* 10‰ fluctuation of $\delta^{18}O$ resulting in very low values (down to 11‰) is highly unlikely to be of a primary depositional

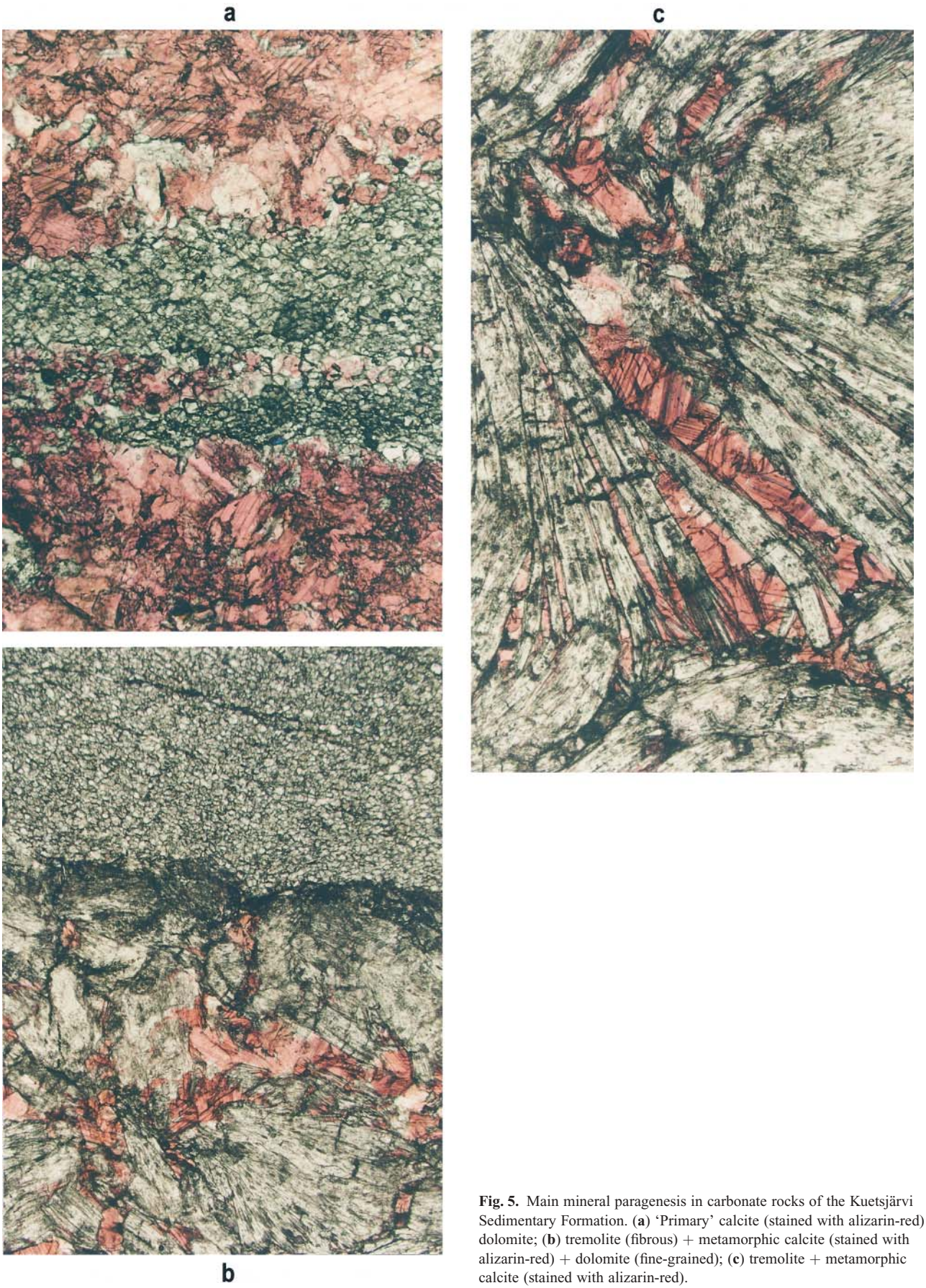

Fig. 5. Main mineral paragenesis in carbonate rocks of the Kuetsjärvi Sedimentary Formation. (**a**) 'Primary' calcite (stained with alizarin-red) + dolomite; (**b**) tremolite (fibrous) + metamorphic calcite (stained with alizarin-red) + dolomite (fine-grained); (**c**) tremolite + metamorphic calcite (stained with alizarin-red).

Table 2. *$\delta^{13}C$ and $\delta^{18}O$ analyses of bulk carbonates from tremolite–calcite–dolomite rocks in the Superdeep Drillhole*

Analysis number	Sample number	Rock	δ^{13}C (‰)	δ^{18}O (‰)
1	5647	Tremolite–calcite–dolomite rock	+2.6	10.6
2	5659	Tremolite–calcite rock	+1.2	11.1
3	5662.7	Tremolite–calcite rock	+3.1	12.6
4	5668	Tremolite–calcite–dolomite rock with talc and phlogopite	+4.6	13.0
5	5671.55	Tremolite–calcite–dolomite rock	+7.2	13.5
6	5671.7	Tremolite–calcite–dolomite rock	+3.2	12.2
7	5687	Tremolite–calcite–dolomite rock with phlogopite	+6.5	14.2
8	5692	Tremolite–calcite–dolomite–quartz rock with apatite	+6.0	11.5
9	5694	Tremolite–calcite–dolomite–quartz rock with apatite	+5.9	11.9
10	5696.2	Quartz–phlogopite schist with calcite	+7.3	13.2
11	5697.9	Quartz–microcline–phlogopite schist with calcite	+3.3	7.3
12	5701	Quartz–microcline–phlogopite schist with calcite	+3.5	12.0
13	5706.2	Calcite-cemented arkosic sandstone with epidote	−2.4	14.5
14	5708.1	Calcite-cemented arkosic sandstone	+3.4	9.9
15	5708.95	Calcite-cemented arkosic sandstone	+3.9	8.8

Table 3. *$\delta^{13}C$ and $\delta^{18}O$ in Superdeep Drillhole carbonates within thin section scale; samples obtained by microcoring*

Sample number	Mineral	δ^{13}C (‰)	δ^{18}O (‰)
'*Primary*' *calcite–dolomite association, depth 5670.0 m*			
1	Dolomite	+6.8	12.5
2	'Primary' calcite	+6.7	13.3
3	Dolomite	+7.4	12.8
4	'Primary' calcite	+6.8	13.2
5	Dolomite	+7.5	12.3
6	'Primary' calcite	+6.7	13.1
7	Dolomite	+7.0	12.4
8	'Primary' calcite	+6.7	13.1
9	Dolomite	+7.5	12.6
10	'Primary' calcite	+5.5	13.3
11	Dolomite	+7.4	12.8
12	'Primary' calcite	+6.7	14.1
Average, dolomite		$+7.3 \pm 0.3$	12.6 ± 0.2
Average, 'primary' calcite		$+6.5 \pm 0.5$	13.4 ± 0.4
Average, $\Delta_{dol-cal}$		+0.8	−0.8
Metamorphic calcite–dolomite association, depth 5686.3 m			
1	Dolomite	+7.5	13.7
2	Metamorphic calcite	+5.2	13.5
3	Dolomite	+6.9	12.9
4	Metamorphic calcite	+5.0	13.6
5	Dolomite	+7.0	13.4
6	Metamorphic calcite	+4.2	13.5
7	Dolomite	+6.9	13.4
8	Metamorphic calcite	+4.0	15.2
9	Metamorphic calcite	+5.0	13.2
Average, dolomite		$+7.1 \pm 0.3$	13.3 ± 0.4
Average, metamorphic calcite		$+4.7 \pm 0.5$	13.8 ± 0.8
Average, $\Delta_{dol-cal}$		+2.4	−0.5

nature. Taking an extreme stance and assuming that the entire δ^{13}C range observed in the most completely sampled section (i.e. drillhole X, +6 to +9‰, Melezhik & Fallick 1996) was caused by depositional factors, then the variation documented outside this range (−1.0 to +6‰) should have a different origin.

Variations of isotopic composition: decarbonation v. isotopic mixing and exchange

One obvious process that could have caused the isotopic resetting is decarbonation reactions. If a rock devolatilizes in a closed system (Nabelek *et al*. 1984; Brown *et al*. 1985) depletion in ^{13}C will vary directly with the amount of devolatilization in accord with mass balance (Valley 1986):

$$\delta^{f} = \delta^{i} - (1 - F)1000\ln\alpha$$

where F is the mole fraction of the element of interest that remains in the rock after devolatilization; α is the isotope fractionation factor (fluid − rock); δ^{f} and δ^{i} are the initial and final isotopic values of the rock in standard per mil notation. Assuming premetamorphic $\delta^{18}O^{i}$ of the Kuetsjärvi Sedimentary Formation dolostones was +20‰, $\alpha = 1.006$, and $F \geqslant 0.6$,

Table 4. *$\delta^{13}C$, $\delta^{18}O$, $\Delta^{13}C_{dol-cal}$ and $\Delta^{18}O_{dol-cal}$ values measured from microcored calcite and dolomite samples obtained from tremolite–calcite–dolomite rocks in the Superdeep Drillhole*

Analysis number	Sample number	Mineral	$\delta^{13}C$ (‰)	$\delta^{18}O$ (‰)	$\Delta^{13}C_{dol-cal}$ (‰)	$\Delta^{18}O_{dol-cal}$ (‰)
1	5659.8	Dolomite	+6.1	13.6		
2	5660.8a	Metamorphic calcite	+3.8	16.5		
3	5660.8b	Vein calcite	−1.0	12.4		
4	5661.6	Dolomite	+5.8	12.8		
5	5662.4a	Dolomite	+6.0	12.5	+0.7	−2.1
6	5662.4b	Metamorphic calcite	+5.3	14.6		
7	5663.0	Dolomite	+5.5	11.0		
8	5665.0	Metamorphic calcite	+4.5	12.8		
9	5668.0	Metamorphic calcite	+5.4	16.9		
10	5669.65a	Dolomite	+5.4	16.5	+0.2	+2.7
11	5669.65b	Metamorphic calcite	+5.8	13.2		
12	5670[1]	Dolomite	+7.3	12.6	+0.8	−0.8
13	5670[1]	'Primary' calcite	+6.5	13.4		
14	5671.1b	Dolomite	+7.1	13.2	+2.4	+0.4
15	5671.1a	Metamorphic calcite	+4.7	12.8		
16	5671.55	Dolomite	+6.9	13.1		
17	5671.9	Metamorphic calcite	+5.9	13.5		
18	5674.7	Dolomite	+7.2	13.7		
19	5681.6a	Micritic dolomite	+7.5	13.6		
20	5681.6b	Sparry dolomite	+8.2	14.8		
21	5681.6c	Metamorphic calcite	+5.9	14.9		
22	5681.7	Dolomite	+7.8	15.1		
23	5681.8	Dolomite	+7.7	14.6		
24	5682.0	Dolomite	+7.2	14.0		
38	5682.2a	Dolomite	+7.4	14.1	+2.2	−0.1
39	5682.2b	Metamorphic calcite	+5.2	14.2		
25	5683.6	Dolomite	+7.2	14.2		
26	5685.0	Dolomite	+7.2	14.3		
27	5685.1	Dolomite	+7.5	15.0		
28	5685.35b	Dolomite	+7.9	14.3	+2.3	+0.4
29	5685.35a	Metamorphic calcite	+5.6	13.9		
30	2685.65b	Dolomite	+7.8	14.4	+3.7	+0.5
31	2685.65a	Metamorphic calcite	+4.1	13.9		
32	5685.85b	Micritic dolomite	+7.5	13.3		
33	5685.85a	Sparry dolomite	+7.8	13.6		
34	5685.95b	Dolomite	+6.6	13.6	+1.9	−0.5
35	5685.95a	Metamorphic calcite	+4.7	14.1		
36	5686.1a	Dolomite	+7.3	13.8	+2.7	−0.2
37	5686.1b	Metamorphic calcite	+4.6	14.0		
40	5686.3	Dolomite	+7.4	13.8		
41	5686.5	Metamorphic calcite	+4.6	14.1		
42	5686.3[1]	Dolomite	+7.1	13.3	+2.4	−0.5
43	5686.3[1]	Metamorphic calcite	+4.7	13.8		
44	5686.8	Dolomite	+7.2	13.3		
45	5687.2a	Dolomite	+6.9	12.9	+2.3	+0.1
46	5687.2b	Metamorphic calcite	+4.6	12.8		
47	5688.2a	Dolomite	+7.2	11.9	+3.6	−0.1
48	5688.2b	Metamorphic calcite	+3.6	12.0		
49	5688.3	Dolomite	+6.2	12.0		

[1]Average values based on data from Table 3.

which is a calc-silicate limit for most metamorphic reactions (e.g. Valley 1986), the 'batch' devolatilization model of probable decarbonation reactions predicts a maximum ^{18}O depletion of the order of 2.5‰.

Isotopic resetting in an 'open-system devolatilization' (Rayleigh 1896; Epstein 1959; Brown *et al*. 1985) as a result of Rayleigh distillation is quantified by

$$\delta^{f} = \delta^{i} + 10^{3}(F^{\alpha-1} - 1).$$

This predicts a maximum ^{18}O depletion of the order of 3‰. Thus, neither of the models described above can account for the significant ^{18}O depletion observed in all samples excluding biotite-actinolite-facies data from the surface outcrops (Fig. 6a). The most probable explanation of considerable depletion in ^{18}O is the loss of ^{18}O-enriched fluids during decarbonation coupled with exchange between the carbonates and fluid with an external source of oxygen, or mixing with internal non-carbonate fluids.

The large depletion in ^{18}O of dolomites from drillhole X with respect to the similar metamorphic grade dolostones sampled from surface is clearly associated with an enhanced fluid flux within the tectonic block, which experienced post-peak metamorphic brecciation and shearing (D_3). The positive correlation between $\delta^{18}O$ and the carbonate content (Fig. 8b) indicates that the oxygen isotopic composition was partially buffered by pre-

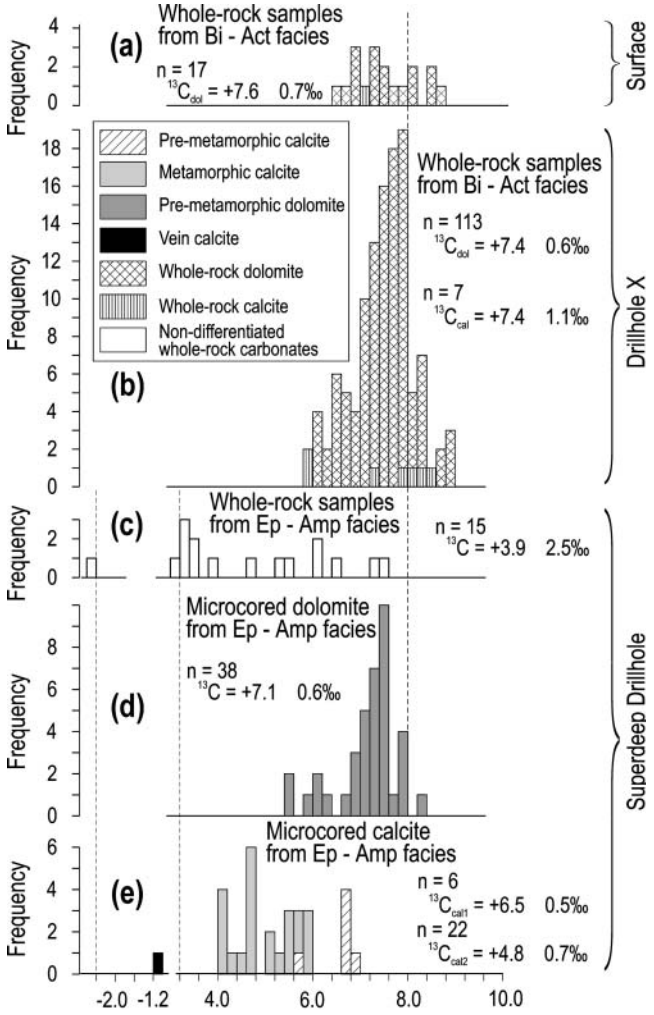

Fig. 6. $\delta^{13}C_{carb}$ v. metamorphic facies. Data from surface outcrops and drillhole X are from Melezhik & Fallick (1996).

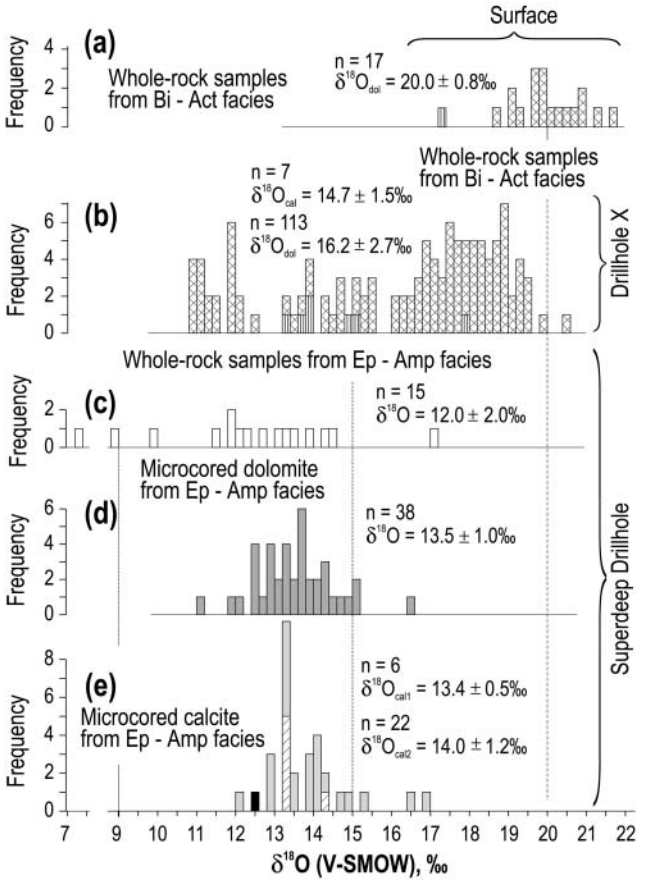

Fig. 7. $\delta^{18}O_{carb}$ v. metamorphic facies. Data from surface outcrops and drillhole X are from Melezhik & Fallick (1996). Legend as in Figure 6.

existing carbonate. However, significantly different gradients observed for the lower $\delta^{18}O$ ($r = 0.63$) and higher $\delta^{18}O$ ($r = 0.40$) subsets suggest that the most ^{18}O-depleted dolomite was at a high fluid/rock ratio. The location of such dolomite samples near contacts with non-carbonate lithologies (Fig. 8a) is consistent with enhanced infiltration of fluids having an external source of oxygen (i.e. not determined by interaction with carbonate). A symmetrical depletion of the dolomite body in ^{18}O towards the most permeable brecciated and sheared zones (Fig. 8a) can also be explained by infiltration of fluids with an external source of oxygen. The formation of chlorite veinlets is evidence of such foreign fluids, their composition suggesting a mafic source. Thus, the isotopic pattern observed in Fig. 8a suggests that nearly all dolomite samples, apart from a few with $\delta^{18}O$ fluctuating around 20‰, were affected by isotopic exchange with fluids. The magnitude of the isotopic resetting can be comparable with that documented in the epidote-amphibolite-facies dolomite (Fig. 7c–e). The bulk of the rocks, however, escaped a pervasive isotopic resetting, and $\delta^{18}O$ was partially buffered by the pre-existing dolomite. Nevertheless, only very few samples retained the isotopic signature ($\delta^{18}O$ *c.* 20‰) close to those measured for the surface dolostones, which were not affected by the intensive brecciation and shearing (Fig. 7a).

A Rayleigh distillation process is especially effective in ^{13}C depletion of carbonates undergoing decarbonation. If both the original ($\delta^{13}C^{i}$) and final ($\delta^{13}C^{f}$) values of carbon isotopes and the amount of CO_2 remaining in the rock (F) are known, it is possible to calculate the time-integrated average fractionation factor (α – fluid–rock) during decarbonation (Nabelek *et al.* 1984):

$$\alpha = \frac{\ln\left(\frac{1000+\delta^{13}C^{f}}{1000+\delta^{13}C^{i}}\right)}{\ln F} + 1.$$

The fraction of CO_2 remaining (F) can be determined from the known amounts of CO_2, CaO and MgO in each sample because dolomite was essentially the only mineral that originally contained calcium and magnesium. Assuming $\delta^{13}C^{i}$ of the Kuetsjärvi Sedimentary Formation dolostones was +8‰, α can be calculated. When α is known, $\Delta^{13}C_{(CO2-carb)}$ can also be calculated:

$$\Delta^{13}C_{(CO_2-carb)} = 10^3 \ln\alpha.$$

Although a Rayleigh distillation process can account for ^{13}C depletion observed in microcored dolomite and calcite$_2$ samples from the epidote-amphibolite facies in the Superdeep Drillhole section (Fig. 7), the calculated α values for the whole-rock samples show a very large variation (1.001–1.045, Table 5) and unrealistically high $\Delta^{13}C_{(CO_2-carb)}$ values (14–44). Kinetic fractionation during decarbonation may explain some of the variation observed in the fractionation factor; however, overall highly

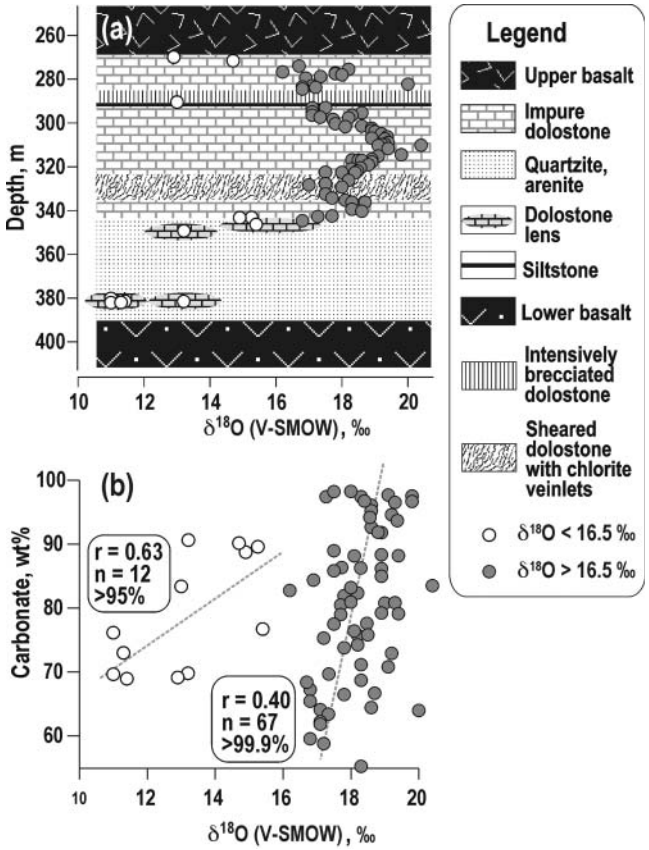

Fig. 8. $\delta^{18}O_{carb}$ v. stratigraphy (**a**) and $\delta^{18}O_{carb}$ v. carbonate content (**b**) for the dolostones from drillhole X. Analytical data are from Melezhik & Fallick (1996).

variable α and $\Delta^{13}C_{(CO_2-carb)}$ values in samples that are from identical metamorphic facies do not agree with the Rayleigh distillation process with no additional source of carbon. Thus, the observed degree of $\delta^{13}C$ and $\delta^{18}O$ variations in whole-rock samples from the Superdeep Drillhole section requires an external source of carbon. The almost total disappearance of alkalis at more-or-less constant Al content in the epidote-amphibolite rocks with respect to their presumed lower-grade equivalents (Table 1) is compatible with fluid infiltration. The observed limited CO_2 lost, combined with considerable depletion in ^{13}C in several samples (Table 5) suggests that the external source should be depleted in ^{13}C. Given the fact that initial carbon isotopic ratios are very high (+8‰), common metamorphic fluids might be applicable for the isotopic resetting of the carbonates from the Superdeep Drillhole section. Non-homogeneous isotopic resetting is also expected because the Kuetsjärvi Sedimentary Formation dolostones are characterized by very variable impurity and different scale layering and lamination. These lithological characteristics might have introduced a highly variable permeability and, consequently resulted in an irregular fluid flux causing different degrees of isotopic exchange with carbonates.

The presence of post-peak metamorphic calcite veinlets that are considerably depleted in both ^{13}C and ^{18}O (Figs 6e and 7e), is considered as direct evidence for late fluids whose isotopic composition was influenced by factors external to the system. These later fluids may be responsible for the most significant depletion in ^{13}C ($\delta^{13}C < +4‰$, Fig. 6c) and in ^{18}O ($\delta^{18}O < 12‰$, Fig. 7c) observed in the whole-rock samples.

Depositional isotopic values in Superdeep Drillhole carbonates

Assuming that the highest $\delta^{18}O$ value of 22‰ obtained from the surface sample is the least altered value, all $\delta^{18}O$ values measured from drillhole X and Superdeep Drillhole samples (Fig. 5b–e) have been be affected by alteration and thus do not reflect primary depositional environments.

The whole-rock samples from Superdeep Drillhole (if two exceptions are excluded) are significantly depleted in ^{13}C. $Calcite_2$ from the Superdeep Drillhole section is depleted by 2–4‰ as compared with the least altered $\delta^{13}C$ value of +8‰. $\delta^{13}C$ histograms and average carbon isotope values of dolomite from the surface and drillhole X are rather similar to those measured from Superdeep Drillhole section. However, when data are plotted against stratigraphic position it becomes evident that all microcored dolomite samples from the Superdeep Drillhole section, with very few exceptions, are also depleted in ^{13}C as compared with the drillhole X section (Fig. 4). The 1–2‰ subparallel isotopic shift of the Superdeep Drillhole microcored dolomite towards lower values fits well with a Rayleigh distillation process discussed above. Additionally, the Superdeep Drillhole isotopic profile is much 'noisier' as compared with that documented in drillhole X. Fluctuations outside the range of 1–2 might be attributed to the degree of decarbonation, which is, in turn, controlled by a dolomite/quartz ratio, or local kinetic disequilibrium.

Table 5. *Calculated values of the amount of decarbonation,* $\Delta^{13}C_{(CO_2-carb)}$ *and fluid/rock ratios*

Sample number	wt% MgO	wt% CaO	wt% CO_2	$\delta^{13}Cf$	mol% MgO	mol% CaO	mol% CO_2	CO_2 necessary	CO_2 lost	CO_2 remained F	α	$\Delta^{13}C_{(CO_2-carb)}$
5647	17.5	28.9	28.7	+2.6	434	515	652	949	297	0.69	1.014	14.4
5659	20.2	28.3	38.0	+1.2	501	504	864	1006	142	0.86	1.045	44
5662.7	19.7	26.9	34.6	+3.1	489	480	786	968	182	0.81	1.023	22.9
5668	20.1	24.8	18.9	+4.6	499	442	430	941	511	0.46	1.004	4.3
5671.55	22.5	28.9	42.4	+7.2	558	515	964	1073	110	0.90	1.008	7.5
5671.7	22.5	19.0	7.4	+3.2	558	339	168	897	729	0.19	1.003	2.9
5687	21.2	20.9	13	+6.5	526	373	295	899	603	0.33	1.001	1.3

Conclusions

(1) The Paleoproterozoic ^{13}C-rich dolostones, representing a global perturbation of terrestrial carbon cycle, underwent progressive metamorphism followed by a localized retrograde alteration. The combination of nearby samples from the Kola Superdeep Drillhole (12 262 m), the deep drillhole X (1060 m) and the surface provided a unique opportunity for direct tracing of carbon and oxygen isotope fractionation through the low- to high-grade greenschist-facies transition within the same formation of impure dolostones accumulated in an intracratonic setting.

(2) Primary mineral parageneses include dolomite + $calcite_1$ + quartz ± K-feldspar. The transition from biotite-actinolite to epidote-ampibolite facies is defined by dolomite + quartz → tremolite + $calcite_2$ ± dolomite ± $calcite_1$. The retrograde alteration is expressed by the formation of quartz–chlorite veinlets within brecciated and sheared dolostones.

(3) The least-altered dolostones from the low-grade greenschist facies yield $\delta^{13}C$ values of +9‰ and $\delta^{18}O$ values of 22‰. The transition from biotite-actinolite to epidote-ampibolite facies is characterized by the formation of $calcite_2$ and recrystallization of $calcite_1$ and dolomite. The transition is defined by ^{13}C depletion of $calcite_2$ (*c*. 3.0‰) and $calcite_1$ (1.0–2.0‰) associated with a Rayleigh distillation process. The dolomite is depleted in ^{13}C by <1‰. In contrast, the oxygen isotopes show a considerable resetting in all carbonate components of the order of 6‰ caused by a Rayleigh distillation process coupled with isotopic exchange between the carbonates and fluids with an external source of oxygen.

(4) Most of the low-grade greenschist-facies dolostones of drillhole X experienced ^{18}O depletion by 1–2‰, but the maximum depletions in dolomite (*c*. 9‰) and $calcite_1$ (*c*. 7‰) were probably controlled by the infiltration of external fluids into permeable zones (on the scale of a few metres). $\delta^{13}C$ remains largely unaffected.

(5) The least altered $\delta^{13}C$ values of impure dolostones from epidote-amphibolite facies may be provided by analyses of microcored dolomite samples, whereas whole-rock and microcored $calcite_2$ are considerably depleted in ^{13}C and cannot be used as the proxy for primary depositional signature.

This research forms part of IGCP Project No. 408 and was funded by the Geological Survey of Norway (Project 282200). The isotope analyses were performed at the Scottish Universities Environmental Research Centre supported by the Consortium of Scottish Universities and the Natural Environment Research Council. P. Robinson read an earlier version of the manuscript and suggested improvements, for which we are grateful. A. C. Barnicoat and an anonymous referee helped us to focus on the most important topic and to make the manuscript intelligible.

References

Amelin, Yu.V., Heaman, L.M. & Semenov, V.S. 1995. U–Pb geochronology of layered mafic intrusions in the eastern Baltic Shield: implications for the timing and duration of Palaeoproterozoic continental rifting. *Precambrian Research*, **75**, 31–46.

Baker, A.J. & Fallick, A.E. 1989a. Evidence from Lewisian limestone for isotopically heavy carbon in two-thousand-million-year-old sea water. *Nature*, **337**, 352–354.

Baker, A.J. & Fallick, A.E. 1989b. Heavy carbon in two-billion-year-old marbles from Lofoten–Vesterålen, Norway: implications for the Precambrian carbon cycle. *Geochimica et Cosmochimica Acta*, **53**, 1111–1115.

Bakushkin, Ye.M. & Akhmedov, A.M. 1975. Basal conglomerate of the Pechenga Complex near the Mt. General'skaya. *In:* Bel'kov, I.V. (ed.) *Geology and Geochemistry of the Metamorphic Complexes of the Kola Peninsula*. Kola Science Centre, Apatity, **70-77**, 70–77 (in Russian).

Balashov, Yu.A. 1996. Geochronology of Early Proterozoic rocks from the Pechenga/Varzuga structure in the Kola Peninsula. *Petrology*, **4**, 3–25 (in Russian).

Banner, J.L. & Hanson, G.N. 1990. Calculation of simultaneous isotopic and trace element variations during water–rock interaction with applications to carbonate diagenesis. *Geochimica et Cosmochimica Acta*, **54**, 3123–3137.

Brown, P.E., Bowman, J.R. & Kelly, W.C. 1985. Petrologic and stable isotope constraints on the source and evolution of skarn-forming fluids in Pine Creek, California. *Economic Geology*, **80**, 72–95.

Baumgartner, L.P. & Valley, J.W. 2001. Stable isotope transport and contact metamorphic fluid flow. *In:* Valley, J.W. & Cole, D.R. (eds) *Stable Isotope Geochemistry*. Reviews in Mineralogy and Geochemistry, **43**, 445–489.

Duk, G.G. 1977. *Structural–Metamorphic Evolution of the Pechenga Complex*. Nauka, Leningrad (in Russian).

Epstein, S. 1959. The variations of the $^{18}O/^{16}O$ ratios in nature and some geologic implications. *In:* Abelson, P.H. (ed.) *Researches in Geochemistry*. Wiley, New York, 217–240.

Ghent, E.D. & O'Neil, J.R. 1985. Late Precambrian marbles of unusual carbon-isotope composition, southeastern British Columbia. *Canadian Journal of Earth Sciences*, **22**, 324–329.

Glagolev, A.A., Kazansky, V.I., Prokhorov, K.V., Rusinov, V.L., Maslennikov, V.A., Voronovsky, S.N. & Ovchinnikov, L.N. 1987. Zonality and age of metamorphism. *In:* Kozlovsky, Ye.A. (ed.) *The Superdeep Well of the Kola Peninsula*. Springer, Berlin, 166–198.

Guerrera, A. Jr, Peacock, S.M. & Knauth, L.P. 1997. Large ^{18}O and ^{13}C depletions in greenschist facies carbonate rocks, western Arizona. *Geology*, **25**, 943–946.

Hanski, E., Huhma, H., Smol'kin, V.F. & Vaasjoki, M. 1990. The age of ferropicritic volcanites and comagmatic Ni-bearing intrusions at Pechenga, Kola Peninsula, U.S.S.RÒ *Geological Society of Finland Bulletin*, **62**, 123–133.

Lanev, V.S. & Nalivkina, E.B. *et al.*1987. Geological section of the well. *In:* Kozlovsky, Ye.A. (ed.) *The Superdeep Well of the Kola Peninsula*. Springer, Berlin, 40–73.

Marker, M. 1985. Early Proterozoic (*c*. 2000–1900 Ma) crustal structure on the north-eastern Baltic Shield: tectonic division and tectonogenesis. *Norges Geologiske Undersøkelse Bulletin*, **403**, 55–74.

McCrea, J.M. 1950. On the isotopic chemistry of carbonates and a paleotemperature scale. *Journal of Chemical Physics*, **18**, 849–857.

Melezhik, V.A. & Fallick, A.E. 1996. A widespread positive ($^{13}C_{carb}$ anomaly at around 2.33–2.06 Ga on the Fennoscandian Shield: a paradox? *Terra Nova*, **8**, 141–157.

Melezhik, V.A. & Sturt, B.A. 1994. General geology and evolutionary history of the early Proterozoic Polmak–Pasvik–Pechenga–Imandra/Varzuga–Ust'Ponoy Greenstone Belt in the north-eastern Baltic Shield. *Earth-Science Reviews*, **36**, 205–241.

Melezhik, V.A. & Sturt, B.A. 1995. The largest Early Proterozoic greenstone belt in the north-eastern Fennoscandian Shield: palaeotectonic significance. *In:* Robert, D. & Nordgulen, Ø. (eds) *Geology of the Eastern Finnmark–Western Kola Peninsula Region*. Norges Geologiske Undersøkelse Special Publication, **7**, 117–118.

Melezhik, V.A., Fallick, A.E., Medvedev, P.V. & Makarikhin, V.V. 1999. Extreme $^{13}C_{carb}$ enrichment in *ca*. 2.0 Ga magnesite–stromatolite–dolomite–'red beds' association in a global context: a case for the world-wide signal enhanced by a local environment. *Earth-Science Reviews*, **48**, 71–120.

Melezhik, V.A., Gorokhov, I.M., Fallick, A.E. & Gjelle, S. 2001. Strontium and carbon isotope geochemistry applied to dating of carbonate sedimentation: an example from high-grade rocks of the Norwegian Caledonides. *Precambrian Research*, **108**, 267–292.

Melezhik, V.A., Sturt, B.A., Ramsay, D.M., Nilsson, L.-P. & Balashov, Yu.A. 1995. The early Proterozoic Pasvik–Pechenga Greenstone Belt: 1:200,000 geological map, stratigraphic correlation and revision in stratigraphic nomenclature. *In:* Robert, D. & Nordgulen, Ø. (eds) *Geology of the Eastern Finnmark–Western Kola Peninsula Region*. Norges Geologiske Undersøkelse Special Publication, **7**, 81–93.

Mintz, M.V. 1993. Palaeotectonic reconstruction of the Early Precambrian in the Eastern Baltic Shield, Part 1: Early Proterozoic. *Geotectonica*, **1**, 39–56 (in Russian).

Nabelek, P.I. 1991. Stable isotope monitors. *In:* Kerrick, D.M. (ed.) *Contact Metamorphism*. Mineralogical Society of America, Reviews in Mineralogy, **26**, 395–435.

Nabelek, P.I., Labotka, T.C., O'Neil, J.R. & Papike, J.J. 1984. Contrasting fluid/rock interaction between the Notch Peak granitic intrusion and argillites and limestones in western Utah: evidence from stable isotopes and phase assemblages. *Contributions to Mineralogy and Petrology*, **86**, 25–34.

Petrov, V.P. & Voloshina, I.M. 1995. Regional metamorphism of the Pechenga area rocks. *In:* Mitrofanov, F.P. & Smol'kin, V.F. (eds) *Magmatism, Sedimentogenesis and Geodynamics of the Pechenga Palaeorift*. Kola Science Centre, Apatity, 164–182 (in Russian).

Rayleigh, J.W.S. 1896. Theoretical considerations respecting the separation of gases by diffusion and similar processes. *Philosophical Magazine*, **42**, 493.

Rosenbaum, J.M. & Sheppard, S.M.F. 1986. An isotopic study of siderites, dolomites and ankerites at high temperatures. *Geochimica et Cosmochimica Acta*, **50**, 1147–1159.

Sharkov, E. & Smolkin, V.F. 1997. The early Proterozoic Pechenga–Varzuga Belt: a case of back-arc spreading. *Precambrian Research*, **82**, 135–151.

Shieh, Y.N. & Taylor, H.P. 1969. Oxygen and carbon isotope studies of contact metamorphism of carbonate rocks. *Journal of Petrology*, **10**, 307–331.

Taylor, B.E. & O'Neil, J.R. 1977. Stable isotope studies of metasomatic Ca–Fe–Al–Si skarns associated metamorphic and igneous rocks, Osgood Mountains, Nevada. *Contributions to Mineralogy and Petrology*, **63**, 1–49.

Valley, J.W. 1986. Stable isotope geochemistry of metamorphic rocks. *In:* Valley, J.W., Taylor, H.P. & O'Neil, J.R. (eds) *Stable Isotopes in High Temperature Geological Processes*. Mineralogical Society of America, Reviews in Mineralogy, **16**, 445–489.

Valley, J.W. & O'Neil, J.R. 1984. Fluid heterogeneity during granulite facies metamorphism in the Adirondacks: stable isotope evidence. *Contributions to Mineralogy and Petrology*, **85**, 158–173.

Veizer, J. 1983a. Trace elements and isotopes in sedimentary carbonates. *In:* Reeder, R.J. (ed.) *Carbonates: Mineralogy and Chemistry*. Mineralogical Society of America, Reviews in Mineralogy, **11**, 265–299.

Veizer, J. 1983b. Chemical diagenesis of carbonates: theory and application of the trace element technique. *In:* Arthur, M.A., Anderson, T.F., Kaplan, I.R., Veizer, J. & Land, L.S. (eds) *Stable Isotopes in Sedimentary Geology*. Society for Economic Petrology and Mineralogy Short Course Notes, **10**, 3.1–3.100.

Veizer, J., Clayton, R.N. & Hinton, R.W. 1992a. Geochemistry of Precambrian carbonates: IV. Early Paleoproterozoic (2.25 ± 0.25 Ga) seawater. *Geochimica et Cosmochimica Acta*, **56**, 875–885.

Veizer, J., Clayton, R.N., Hinton, R.W., Von Brunn, V., Mason, T.R., Buck, S.G. & Hoefs, J. 1990. Geochemistry of Precambrian carbonates: III. Shelf seas and non-marine environments of the Archean. *Geochimica et Cosmochimica Acta*, **54**, 2717–2729.

Veizer, J., Plumb, K.A., Clayton, R.N., Hinton, R.W. & Grotzinger, J.P. 1992b. Geochemistry of Precambrian carbonates: V. Late Paleoproterozoic seawater (1.8 ± 0.25 Ga). *Geochimica et Cosmochimica Acta*, **56**, 2487–2501.

Wickham, S.M. & Peters, M.T. 1993. High (^{13}C Neoproterozoic carbonate rocks in western North America. *Geology*, **21**, 165–168.

Winkler, H.G.F. 1979. *Petrogenesis of Metamorphic Rocks*. Springer, Berlin.

Zagorodny, V.G., Mirskaya, D.D. & Suslova, S.N. 1964. *Geology of the Pechenga Sedimentary–Volcanogenic Series*. Nauka, Leningrad.

Zheng, Y. 1997. Oxygen and carbon isotope anomalies in the ultrahigh pressure metamorphic rocks of the Dabi-Sulu terranes: implications for geodynamics. *Episodes*, **20**, 104–108.

Received 25 January 2002; revised typescript accepted 13 August 2002.
Scientific editing by Mike Fowler